SPANDIDOS PUBLICATIONS

INTERNATIONAL JOURNAL OF ONCOLOGY 55: 309-319, 2019

Potent and specific fusion toxins consisting of a HER2-binding, ABD-derived affinity protein, fused to truncated versions of *Pseudomonas* exotoxin A

HAO LIU[1], SARAH LINDBO[1], HAOZHONG DING[1], MOHAMED ALTAI[2], JAVAD GAROUSI[2], ANNA ORLOVA[3], VLADIMIR TOLMACHEV[2], SOPHIA HOBER[1] and TORBJÖRN GRÄSLUND[1]

[1]Department of Protein Science, KTH Royal Institute of Technology, 114 17 Stockholm;
[2]Department of Immunology, Genetics and Pathology, Uppsala University, 751 85 Uppsala;
[3]Department of Medicinal Chemistry, Uppsala University, 751 23 Uppsala, Sweden

Received January 2, 2019; Accepted April 22, 2019

DOI: 10.3892/ijo.2019.4814

Abstract. Fusion toxins consisting of an affinity protein fused to toxic polypeptides derived from *Pseudomonas* exotoxin A (ETA) are promising agents for targeted cancer therapy. In this study, we examined whether fusion toxins consisting of an albumin binding domain-derived affinity protein (ADAPT) interacting with human epidermal growth factor receptor 2 (HER2), coupled to the ETA-derived polypeptides PE38X8 or PE25, with or without an albumin binding domain (ABD) for half-life extension, can be used for specific killing of HER2-expressing cells. The fusion toxins could easily be expressed in a soluble form in *Escherichia coli* and purified to homogeneity. All constructs had strong affinity for HER2 (K_D 10 to 26 nM) and no tendency for aggregation could be detected. The fusion toxins including the ABD showed strong interaction with human and mouse serum albumin [equilibrium dissociation constant (K_D) 1 to 3 nM and 2 to 10 nM, respectively]. The *in vitro* investigation of the cytotoxic potential revealed IC_{50}-values in the picomolar range for cells expressing high levels of HER2. The specificity was also demonstrated, by showing that free HER2 receptors on the target cells are required for fusion toxin activity. In mice, the fusion toxins containing the ABD exhibited an appreciably longer time in circulation. The uptake was highest in liver and kidney. Fusion with PE25 was associated with the highest hepatic uptake. Collectively, the results suggest that fusion toxins consisting of ADAPTs and ETA-derivatives are promising agents for targeted cancer therapy.

Introduction

Immunotoxins are fusion proteins consisting of an Ig-derived targeting domain and a highly toxic protein or peptide. These have been under intense study over the past few decades, and several immunotoxins are under pre-clinical and clinical evaluation (www.clinicaltrials.gov) (1,2). In 2018, the first immunotoxin was approved by the US Food and Drug Administration (FDA), namely moxetumomab pasudotox for the treatment of hairy cell leukemia (3). Fusion proteins, consisting of a toxic protein or peptide coupled to a non-Ig-derived affinity protein are also under evaluation and are denoted fusion toxins (4). One fusion toxin has been approved by the FDA for therapy, namely denileukin diftitox for the treatment of cutaneous T-cell lymphoma (5).

The toxin part of immunotoxins and fusion toxins is often of bacterial or plant origin. A well-studied toxin is PE38, which is a truncated version of *Pseudomonas* exotoxin A (ETA), where domain I, responsible for target cell interaction has been removed. When PE38-containing constructs are internalized, a cleavage by furin occurs in domain II, followed by release into the cytosol. PE38 then exerts its toxic effect through ribosylation of elongation factor 2, effectively preventing further protein synthesis, which leads to cell death. A drawback with PE38-based constructs is the relatively high immunogenicity, limiting the number of consecutive injections possible in animals and humans before anti-drug antibodies are formed (6). Several efforts to decrease the immunogenicity have been undertaken, where B- and T-cell epitopes reactive in humans and mice have been identified and removed (7-10). One of these variants is PE38X8 (10). It has 8 mutations to

Correspondence to: Professor Torbjörn Gräslund, Department of Protein Science, KTH Royal Institute of Technology, Roslagstullsbacken 21, 114 17 Stockholm, Sweden
E-mail: torbjorn@kth.se

Abbreviations: ABD, albumin binding domain; ADAPT, ABD-derived affinity protein; *E. coli*, *Escherichia coli*; ETA, *Pseudomonas* exotoxin A; FcRn, neonatal Fc receptor; GMP, good manufacturing practice; HER2, human epidermal growth factor receptor 2; IMAC, immobilized metal-ion affinity chromatography; IPTG, isopropyl β-D-1-thiogalactopyranoside; ITLC, instant thin layer chromatography; K_D, equilibrium dissociation constant; MSA, mouse serum albumin

Key words: exotoxin A, *Pseudomonas*, ABD-derived affinity protein, half-life extension, cancer, human epidermal growth factor receptor 2

remove mouse B-cell epitopes and has previously been found suitable for fusion with different targeting domains (10-12). Efforts to minimize the size of the deimmunized versions of PE38 have also been undertaken, where a large portion of the translocation domain II has been replaced by a furin cleavage site and a spacer with the amino acid sequence GGS, leading to PE25, a deimmunized and size-decreased variant with a toxicity that is reported to be similar as PE38 (13,14). PE25 has 10 mutations in the catalytic domain III to suppress B- and T-cell epitopes.

In recent years, alternatives to Ig-derived targeting domains have begun to emerge, consisting of small engineered affinity proteins, so-called alternative scaffold proteins (15). They are often based on naturally occurring proteins or protein-domains, and their development has been driven by the notion that antibodies have limitations in different applications. A few fusion toxins, including alternative scaffold proteins have been described in the literature (11,12,16-19), although their properties are relatively unexplored.

Albumin binding domain (ABD)-derived affinity proteins (ADAPTs) are a novel group of alternative scaffold proteins originating from one of the albumin-binding domains (GA148-GA3) of streptococcal protein G (20). These non-immunoglobulin-based ligands fold into a three-helical bundle motif, have no naturally occurring cysteines and usually have high thermal and proteolytic stability. ADAPTs consist of only 46 amino acids, which renders them considerably smaller than the majority of other folded alternative scaffold proteins. Furthermore, in contrast to several other alternative scaffold proteins, the ADAPTs have been designed to allow for bi-specificity by preserving the surface residues interacting with albumin when selecting for novel binders (21). However, for some ADAPTs, the interaction with albumin is not desired and has been removed. Among others, ADAPTs binding to the tumor cell markers, human epidermal growth factor receptor 2 (HER2) and human epidermal growth factor receptor 3 (HER3), have been described (22,23).

HER2 (also known as ErbB2) is a cell surface bound tyrosine kinase receptor that belongs to the human epidermal growth factor receptor family with important roles in cancer development (24). HER2 is a clinically validated target and is often overexpressed in breast, ovarian and gastric cancer, while its expression in normal cells is limited (25). Several HER2 targeted drugs have been approved for clinical use by the FDA e.g., Herceptin (trastuzumab) (26), Perjeta (pertuzumab) (27) and Kadcyla (trastuzumab emtansine) (28).

A group of ADAPTs binding to HER2 has been generated and has been found to interact with the receptor with different affinities (23). The most studied variant, $ADAPT_6$, is a ligand targeting domain IV of HER2 with an equilibrium dissociation constant (K_D) of 0.5 nM. The natural affinity for serum albumin in this variant has been removed.

The small sizes of ADAPTs that do not have affinity for albumin, such as $ADAPT_6$, are associated with short *in vivo* half-lives due to rapid renal clearance. When used for *in vivo* molecular imaging, where rapid target accumulation in combination with rapid clearance of unbound molecules is desirable, this feature has proven to be highly beneficial. $ADAPT_6$ has been investigated as a radionuclide molecular imaging agent and appears to be a promising imaging agent for visualization of HER2 expression in human tumors implanted in mice (29,30). However, for therapeutic applications, a short residence time in circulation often correlates with the need for multiple injections, which limits the applicability of small proteins. Hence, strategies to extend the *in vivo* half-life of small protein therapeutics have been developed. One strategy is to fuse the targeting molecule to an albumin-binding moiety to increase the size of the construct *in vivo* by non-covalent association with albumin. Thereby the cut-off size of glomerular filtration in the kidneys can be exceeded. Association with serum albumin also takes advantage of the long serum half-life of albumin, mediated by the interaction with the neonatal Fc receptor (FcRn). The same albumin-binding domain used for development of ADAPTs has been reported as fusion partner of several protein-therapeutics, for half-life extension (31-33). Furthermore, affinity-improved variants of this domain have been developed, where ABD_{035} with its femtomolar affinity for human serum albumin (HSA) has shown to further prolong the serum half-life (20).

In this study, fusion toxins were created, consisting of $ADAPT_6$ coupled to truncated versions of ETA (PE38X8 or PE25), with or without ABD_{035}. Biochemical characterization, including toxicity to cell lines with differential HER2 expression levels, was performed and revealed highly potent fusion toxins with exquisite specificity for cell lines expressing the HER2 receptor. The biodistribution in mice was also investigated.

Materials and methods

General. All chemicals were from Sigma-Aldrich or Merck unless otherwise stated. Restriction enzymes were from New England Biolabs.

Gene construction. The gene encoding $ADAPT_6$-ABD-PE25 with the N-terminal amino acid sequence MHEHEHEDANS was synthesized by Thermo Fisher Scientific and delivered in the pMK-RQ vector (Novagen). The gene was sub-cloned into the expression vector, pET-26b(+) (Novagen), with *Nde*I and *Xho*I restriction enzymes surrounding the gene, resulting in the vector, pET26-$ADAPT_6$-ABD-PE25. The construct also included a *Bam*HI restriction site between the gene fragments encoding $ADAPT_6$ and the ABD, as well as two *Nco*I restriction sites surrounding the gene fragment encoding the ABD domain. The ABD used in this study was ABD_{035}, an engineered version with improved affinity for HSA (34). The gene fragment encoding PE25 was derived from a deimmunized version of PE38 with the following amino acid alterations: R427A, F443A, D463A, R467A, L477H, R490A, R494A, R505A, R538A and L552E, and the deletion of the majority of domain II (Δ251-273 and Δ285-394) (10). A furin cleavage site was placed at the N-terminus of PE25 and it was connected to domain III of PE25 with the amino acids GGS. The expression vector for $ADAPT_6$-PE25 was created by the digestion of pET26-$ADAPT_6$-ABD-PE25 with *Nco*I followed by re-ligation of the vector. The expression vector for $ADAPT_6$-ABD-PE38X8 was created by isolation of the gene fragment encoding $ADAPT_6$ by restriction digestion of pET26-$ADAPT_6$-ABD-PE25 with *Nde*I and *Bam*HI, followed by ligation with the expression vector encoding $Z_{HER2:2891}$-ABD-PE38X8, which had been cut with the same

enzymes, replacing $Z_{HER2:2891}$ (11). The expression vector for Z_{Taq}-ABD-PE25 was created by replacing the gene fragment encoding $ADAPT_6$ in pET26-$ADAPT_6$-ABD-PE25 with the gene encoding Z_{Taq} (35), using the *Nde*I and *Bam*HI restriction sites. All connections between all domains in the constructs included linkers with the amino acids sequence $(S_4G)_3$. All constructs were verified by DNA sequencing. The vector containing the gene for expression of free HEHEHE-DANS-$ADAPT_6$ (36), not fused to any peptides, was included for blocking experiments.

Protein expression and purification. Escherichia coli (*E. coli*) [BL21 Star (DE3)] (Thermo Fisher Scientific) was used for expression of the fusion toxins and free $ADAPT_6$. Cells harboring the expression plasmids were grown in 500 ml cultures in tryptic soy broth supplemented with 5 g/l yeast extract at 37˚C until OD_{600} reached 1.5, after which protein expression was induced by isopropyl β-D-1-thiogalactopyranoside (IPTG; Appolo Scientific) at a concentration of 1 mM. Protein expression was carried out for 2.5 h after which the cells were harvested by centrifugation (4˚C, 7,000 x g, 10 min). *E. coli* cells expressing $ADAPT_6$-PE25 were resuspended in 20 ml loading buffer (300 mM NaCl, 50 mM Na-phosphate, pH 7.0) supplemented with Complete EDTA-free protease inhibitor cocktail (Roche Diagnostics) and lysed by sonication (Sonics VCX-750; Sonics & Material). $ADAPT_6$-PE25 was purified from the supernatant by immobilized metal-ion affinity chromatography (IMAC) on a Ni-Sepharose 6 Fast Flow resin (GE Healthcare) under native conditions according to the manufacturer's protocol with imidazole elution. The eluted material was pooled and diluted 5 times with deionized water. Subsequently, the material was loaded on an anion exchange HiTrap Q HP column (1 ml; GE Healthcare). The running buffer had the following composition: 60 mM NaCl, 10 mM Na-phosphate, pH 7.0. Bound material was eluted by a NaCl-gradient from 0.06 to 1 M. The fractions containing $ADAPT_6$-PE25 were pooled and buffer was exchanged to PBS (10 mM Na-phosphate, 2.7 mM KCl, 137 mM NaCl, pH 7.4) by passage through a PD-10 desalting column (GE Healthcare).

Cell pellets containing fusion toxins, including the ABD were resuspended in TST-buffer [25 mM tris(hydroxymethyl) aminomethane, 1 mM EDTA, 200 mM NaCl, 0.05% Tween-20, pH 8.0] supplemented with Complete EDTA-free protease inhibitor cocktail and lysed by sonication. The proteins were purified by affinity chromatography on a HiTrap NHS sepharose column (GE Healthcare) with immobilized HSA. The supernatant following sonication was loaded on the column after it had been equilibrated with TST, with subsequent washing of the column with TST. The column was further washed with 5 mM ammonium acetate (pH 5.5) followed by elution with 0.5 M acetic acid. Fractions containing protein were pooled followed by buffer exchange to PBS by passage over a PD-10 column. Protein concentrations were determined by the BCA protein assay kit (Thermo Fisher Scientific). The molecular mass of the fusion toxins was determined by liquid chromatography electrospray ionization mass spectrometry (Agilent Technologies). The samples were diluted to a final concentration of 100 ng/μl in 1X PBS prior to analysis on a Bruker impact II time of flight instrument equipped with an ESI source. The samples were injected via an online connected Dionex UltiMate 3000 ultra-high performance liquid chromatography (UHPLC) system (Thermo Fisher Scientific). The UHPLC was equipped with a ProSwift RP-4H column (1x50 mm, product no. 069477, Thermo Fisher Scientific). The chromatography used for the analysis utilized two solvents: Solvent A (3% acetonitrile, 0.1% formic acid) and solvent B (95% acetonitrile, 0.1% formic acid) and was conducted using a flow rate of 200 μl/min. The gradient used was as follows: 4% solvent B for 2 min, 4-90% solvent B within 6 min, 90% solvent B for 2 min, 90-4% solvent B within 1 min followed by 4% solvent B for 4 min. In order to achieve spray, a capillary voltage of 4.5 kV was applied. The mass spectrometer was run in a positive mode with a mass range from 300 to 3.000 m/z and a scan rate of 1 Hz. Spectra were created by averaging every 2 scans. SDS-PAGE was performed by loading approximately 10 μg sample in each lane of a 4-12% gel, followed by electrophoretic separation. The gel was stained with gelcode blue safe protein stain (Thermo Fisher Scientific). The purities were determined by densitometric analysis of the lanes on the SDS-PAGE gel shown in Fig. 1B. The lanes were visualized using a Chemidoc XRS+ and were analyzed by Image Lab 4.1 software (Bio-Rad laboratories). Free $ADAPT_6$ was purified by heat treatment (90˚C, 10 min) followed by IMAC purification as previously described (36).

Biosensor analysis. A Biacore 3000 and a Biacore T200 instrument (GE Healthcare) were used for biosensor analysis. The extracellular domain of HER2 (Sino Biological) was immobilized on a CM5-chip by amine coupling in sodium acetate buffer at pH 4.5. On a second CM5-chip, HSA (Novozymes) and MSA (Sigma-Aldrich) were immobilized in the same manner. The final immobilization level of the extracellular domain of HER2 was 320 RU. The final immobilization level of HSA and MSA was 265 and 207 RU respectively. Reference flow cells were created on both chips by activation and deactivation. HBS-EP [10 mM 4-(2-hydroxyethyl)-1-piperazineethanesulfonic acid (HEPES), 150 mM NaCl, 3 mM EDTA, 0.05% Tween-20, pH 7.4] was used as running buffer and for dilution of the analytes. All experiments were performed at 25˚C with a flow-rate of 50 μl/min. The surfaces were regenerated after each injection by 10 mM HCl. The kinetic parameters for the interaction between fusion toxins and HER2 was derived from Fig. S1 using Biacore T200 evaluation software (version 2.0) by simultaneously considering single injections of each dilution of the analyte in the dilution series. Each dilution series was injected twice. The kinetic parameters for the interaction between fusion toxins and HSA and MSA was derived from Fig. S2 using Biaevaluation (version 4.1) by simultaneously considering all sensorgrams recorded for single injections of each dilution of the analyte in the dilution series. Each dilution series was injected twice.

A Biacore 8K (GE Healthcare) was used for the biosensor analysis presented in Fig. S3. The extracellular domains of HER2, HSA and MSA were immobilized on flow cell 2 in different channels on a CM5-chip by amine coupling in sodium acetate buffer at pH 4.5. Flow cell 1 in each channel was activated/deactivated and used as reference. The final immobilization levels were as follows: 721 RU (HER2), 945 RU (HSA) and 437 RU (MSA). PBS supplemented with

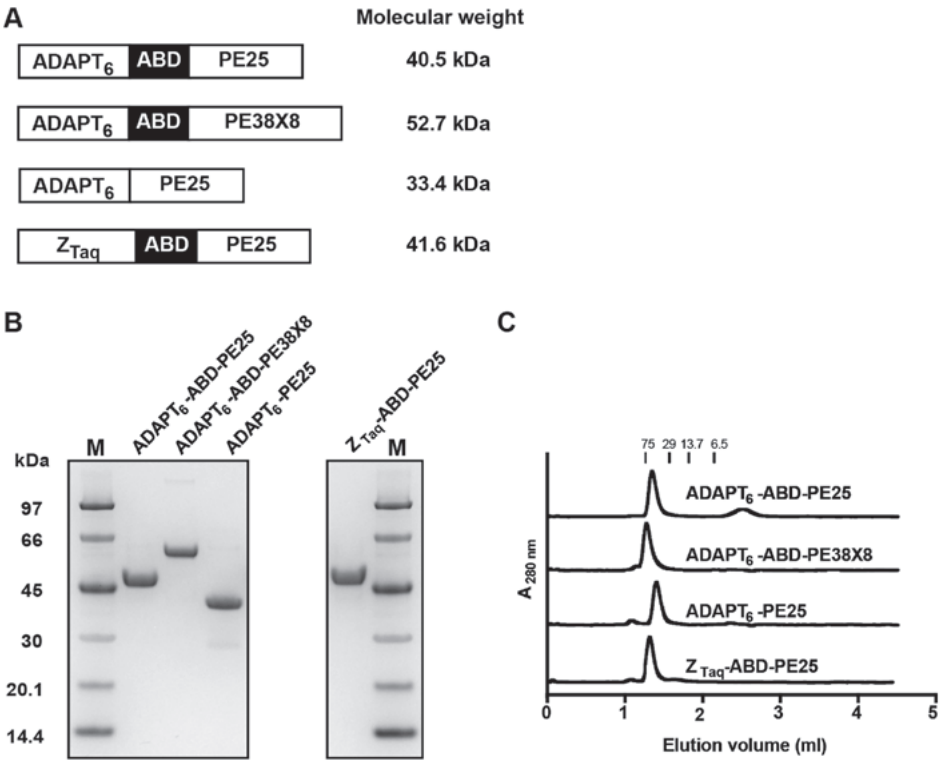

Figure 1. Construction and initial biochemical characterization of the fusion toxins. (A) Schematic representation of the fusion toxins. (B) Purified toxins were analyzed by separation on an SDS-PAGE gel. Numbers to the left are the molecular weights (kDa) of the marker proteins in the two M-lanes. (C) The chromatograms obtained after analytical size-exclusion chromatography of the fusion toxins. The numbers above the chromatograms are the molecular weights (kDa) of protein standards. ADAPT, ABD-derived affinity protein; ABD, albumin binding domain.

0.05% Tween-20 was used for the dilution of the samples and as running buffer.

Cells and cell culture. SKBR3 (breast cancer), AU565 (breast cancer), SKOV3 (ovarian cancer) and A549 (lung cancer) cell lines were obtained from ATCC and were grown in the media recommended: McCoy's 5a or Dulbecco's modified Eagle's medium (Sigma-Aldrich) in a humidified incubator at 37˚C in 5% CO_2 atmosphere. The cell lines were grown for a maximum of 3 months after resuscitation and were routinely tested for mycoplasma infection.

Cytotoxicity of the fusion toxins. To evaluate the cytotoxicity of the fusion toxins on the SKBR3, AU565, SKOV3 and A549 cell lines, approximately 5,000 cells/well were seeded in 96-well plates and were allowed to attach for 4 h. Subsequently, the medium was replaced with fresh medium containing the fusion toxins and the cells were incubated for 72 h at 37˚C, followed by the assessment of cell viability by the measurement of intracellular dehydrogenase activity using a CCK-8 kit according to the manufacturer's protocol (Sigma-Aldrich). The obtained absorbance values were analyzed by Graphpad Prism (Graphpad) to derive IC_{50} values. The data points were fitted with a log (inhibitor) vs. response (4 parameters) function.

Radiolabeling. Purified fusion toxins were conjugated with a benzylisothiocyanate derivative of the CHX-A''-DTPA chelator (Macrocyclics) as previously described (12). In brief, the conjugates were mixed with $^{111}InCl_3$ (8-10 MBq in 20-30 μl 0.05 M HCl) and incubated for 60 min at room temperature. For purification of the radiolabeled conjugates, the mixture was passed through a NAP-5 column pre-equilibrated and eluted with PBS. The radiochemical yield and purity of the conjugates were determined using silica-impregnated ITLC (Instant Thin Layer Chromatography) strips (150-771 DARK GREEN Tec-Control Chromatography strips, Biodex Medical Systems) eluted with 0.2 M citric acid and measured using the Cyclone Storage Phosphor System (PerkinElmer). To evaluate the stability of the labeling, the radiolabeled conjugates were incubated with a 500-fold molar excess of EDTA at room temperature for 4 h, and the percentage of protein-bound radioactivity was determined using radio-ITLC as mentioned above.

Biodistribution. Comparative biodistribution studies of ^{111}In-labeled fusion toxins were performed in 32 female NMRI mice (Taconic M&B Denmark, 8-10 weeks old at arrival). Mice were housed with free access to food and water in rooms with controlled temperature and humidity in an animal facility at Uppsala University. The mice (weighing 25.0±0.7 g) were randomly divided into 8 groups with 4 mice in each group. The animals were injected intravenously with 1 μg (20 kBq) radiolabeled fusion toxin per animal in 100 μl PBS containing 2% BSA. At 4 and 24 h after the injection, the mice were sacrificed by injection of a lethal dose of anesthesia (20 μl of Ketalar-Rompun solution per gram body weight; Ketalar, 200 mg/kg body weight; Rompun, 20 mg/kg body weight, i.p.) followed by heart puncture and exsanguination with a heparinized syringe. Organs and tissue samples were collected, weighed and the radioactivity was measured using an automated gamma-spectrometer. The animal experiments

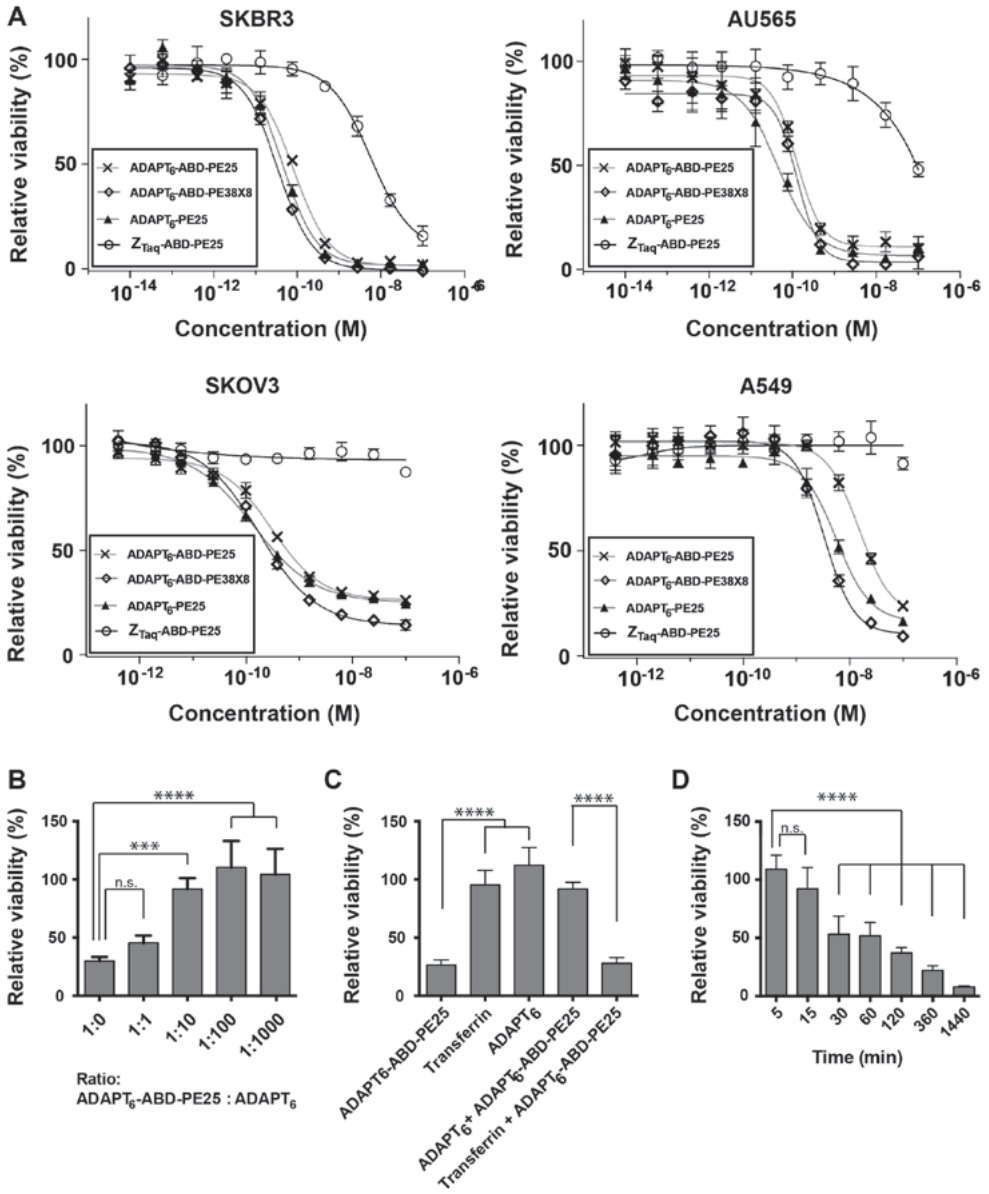

Figure 2. *In vitro* cytotoxicity of the fusion toxins. (A) The cytotoxicity was determined by incubating serial dilutions of the fusion toxins with SKBR3, AU565, SKOV3 and A549 cells. Each data point corresponds to the average of 4 independent experiments. (B) SKOV3 cells were pre-incubated with free $ADAPT_6$ for 5 min followed by the addition of 150 pM $ADAPT_6$-ABD-PE25. Numbers below the panel correspond to the different molar ratios between $ADAPT_6$-ABD-PE25 and $ADAPT_6$. Each data point corresponds to the average measured viability of 4 independent experiments. (C) SKOV3 cells were incubated with (from left to right) 150 pM $ADAPT_6$-ABD-PE25; 15 nM transferrin; 15 nM $ADAPT_6$; cells were pre-incubated with 15 nM $ADAPT_6$ for 5 min followed by the addition of 150 pM $ADAPT_6$-ABD-PE25; cells were pre-incubated with 15 nM transferrin for 5 min followed by addition of 150 pM $ADAPT_6$-ABD-PE25. Each data point corresponds to the mean of four independent experiments. (D) SKOV3 cells were incubated with $ADAPT_6$-ABD-PE25 (3 nM) at the times indicated on the x-axis and then washed 3 times with medium. Fresh medium was added followed by incubation for 72 h. Each data point corresponds to the mean of 4 independent experiments. For each panel, the viability of cells cultivated in growth medium without addition of any toxin was set to 100%. The error bars correspond to 1 SD. Legend to significance indicators: n.s. indicates not significant and corresponds to P>0.05; ***P<0.001 and ****P<0.0001. ADAPT, ABD-derived affinity protein; ABD, albumin binding domain.

were planned and performed in accordance with Sweden's national legislation on laboratory animals' protection. The animal studies were approved by the local ethics committee for animal research in Uppsala, Sweden.

Flow cytometry. To investigate the HER2 expression level in the SKOV3, SKBR3, AU565, and A549 cell lines, $2x10^5$ cells were incubated with trastuzumab obtained in the form of Herceptin (cat. no. 115140, Apoteket) (5 μg/ml) as primary antibody for 30 min, followed by Alexa Fluor 647 conjugated goat anti-human IgG (H+L) (Thermo Fisher Scientific) (cat. no. 1A-21445) (5 μg/ml) as secondary antibody for 30 min. The cells were analyzed on a Gallios flow cytometer (Beckman Coulter). A total of 10,000 events were recorded for each sample and plotted using Kaluza software (Beckman Coulter).

Statistical analysis. Statistical analysis was performed using Prism 8 for macOS (version 8.0.2) (Graphpad). An unpaired two-tailed Student's t-test was used when comparing 2 groups of values. One-way ANOVA with Tukey's (Fig. 2) or Bonferroni's (Table IV) post hoc multiple comparisons

Table I. Biochemical characterization of the fusion toxins.

Fusion toxin	Purity (%)[a]	Calc. Mw (Da)	Found Mw (Da)[b]
$ADAPT_6$-ABD-PE25	99.8	40,549	40,547
$ADAPT_6$-ABD-PE38X8	97.0	52,673	52,669
$ADAPT_6$-PE25	95.1	33,364	33,362
Z_{Taq}-ABD-PE25	99.0	41,554	41,553

[a]From densitometric evaluation of the SDS-PAGE gel in Fig. 1B. [b]The molecular weights were determined by mass spectrometry. Deconvolution was used to determine the monoisotopic mass for each protein.

tests were used when comparing more than 2 groups. The cut-off value for significance was $P<0.05$. The number of repeats/measurements in each group were at least 4. The data are presented as the means ± 1 SD.

Results

Construction, purification and initial biochemical characterization. To investigate the feasibility of utilizing ADAPTs for specific delivery of toxins to cancer cells, two constructs consisting of $ADAPT_6$, specifically targeting the HER2 receptor, coupled to PE25 were produced, with or without an ABD. To investigate the differences between PE25 and PE38X8 as part of a protein fusion with $ADAPT_6$, a third construct consisting of $ADAPT_6$ coupled to ABD and PE38X8 was also produced. As negative control in the *in vitro* experiments, a protein with similar size and fold, Z_{Taq}, was used in lieu of $ADAPT_6$ fused to the ABD and PE25. Z_{Taq} interacts specifically with DNA polymerase from Thermus aquaticus and was not expected to interact with any protein of human origin. A schematic description of all constructs is presented in Fig. 1A.

The fusion toxins were expressed in the cytoplasm of *E. coli*. $ADAPT_6$-PE25 was successfully purified by IMAC followed by anion exchange chromatography. The other constructs, including the ABD, were purified by HSA-based affinity chromatography. Proteins recovered following purification were analyzed by SDS-PAGE and the gel revealed homogenous proteins of the expected molecular weight with a purity between 95.1 and 99.8% (Fig. 1B and Table I).

To investigate the possible formation of aggregates, the purified proteins were analyzed by size-exclusion chromatography under native conditions (Fig. 1C). The elution profiles revealed mono-disperse proteins with a molecular weight of a monomer. Mass spectrometry confirmed the correct molecular masses of the fusion toxins (Table I).

Surface plasmon resonance analysis. The ability of the fusion toxins to interact with HER2 was investigated by biosensor analysis. The dilution series of the fusion toxins were sequentially injected over a surface with immobilized extracellular domain of HER2, to derive the kinetic constants and affinity of the interaction (Table II and Fig. S1). The K_D was similar for $ADAPT_6$-ABD-PE25, $ADAPT_6$-ABD-PE38X8 and $ADAPT_6$-PE25 and ranged from 11 to 26 nM. Z_{Taq}-ABD-PE25, lacking a HER2-binding domain, did not interact with the surface with immobilized HER2 (Fig. S3).

The ability of the ABD-containing fusion toxins to interact with serum albumins was investigated by injection of dilution series over flow cells with immobilized HSA or MSA. The kinetic constants and affinity were derived from the sensorgrams (Table III and Fig. S2). The affinities (K_D) for HSA ranged from 1.1 to 2.2 nM, for the different constructs. The affinities for MSA were slightly weaker and K_D ranged from 3.6 to 6.5 nM. $ADAPT_6$-PE25, lacking an albumin binding domain, did not interact with the surfaces with immobilized HSA or MSA (Fig. S3).

In vitro cytotoxicity. The *in vitro* cytotoxicity was measured by treating SKBR3, SKOV3 and AU565 cells, all with a high HER2 expression (Fig. S4), as well as A549 cells with moderate HER2 expression (Fig. S4), with serial dilutions of the fusion toxins followed by measurement of cell viability. The fusion toxins specifically interacting with HER2 demonstrated picomolar IC_{50} values on SKBR3, SKOV3 and AU565 cells (Fig. 2A). For SKBR3 cells, the IC_{50} values were 84 pM with a 95% confidence interval between 69 and 100 pM ($ADAPT_6$-ABD-PE25), 35 pM with a 95% confidence interval between 30 and 40 pM ($ADAPT_6$-ABD-PE38X8), and 46 pM with a 95% confidence interval between 38 and 56 pM ($ADAPT_6$-PE25). For the AU565 cells the IC_{50} values were 130 pM with a 95% confidence interval between 96 and 170 pM ($ADAPT_6$-ABD-PE25), 130 pM with a 95% confidence interval between 100 and 160 pM ($ADAPT_6$-ABD-PE38X8), and 46 pM with a 95% confidence interval between 31 and 68 pM ($ADAPT_6$-PE25). For SKOV3 cells, the IC_{50} values were 310 pM with a 95% confidence interval between 260 and 370 pM ($ADAPT_6$-ABD-PE25), 180 pM with a 95% confidence interval between 150 and 210 pM ($ADAPT_6$-ABD-PE38X8), and 140 pM with a 95% confidence interval between 120 and 160 pM ($ADAPT_6$-PE25). A comparison of the $ADAPT_6$-ABD-PE25 and $ADAPT_6$-ABD-PE38X8 thus revealed that the fusion toxin, including PE38X8 was slightly more cytotoxic. A comparison of $ADAPT_6$-PE25 with $ADAPT_6$-ABD-PE25, revealed that the inclusion of the ABD lowered the cytotoxicity slightly. The IC_{50} values of the non-target control, Z_{Taq}-ABD-PE25 were found to be 5,700 pM with a 95% confidence interval between 4,100 and 9,100 pM for SKBR3 cells. The relative viability of AU565 and SKOV3 cells at the concentrations used were not affected to such an extent by Z_{Taq}-ABD-PE25 that the IC_{50} values could be measured. The difference in cytotoxicity between the HER2-specific fusion toxins and the Z_{Taq}-control was 2 to

Table II. Affinity constants for fusion toxins interacting with HER2.[a]

Fusion toxin	$k_a/10^4$ (1/Ms)[b]	$k_d/10^{-4}$ (1/s)[b]	$K_D/10^{-8}$ (M)[b]
$ADAPT_6$-ABD-PE25	2.46±0.01	3.68±0.01	1.50±0.01
$ADAPT_6$-ABD-PE38X8	1.06±0.01	2.76±0.03	2.60±0.03
$ADAPT_6$-PE25	4.05±0.01	4.24±0.01	1.05±0.01

[a]The values are derived from the analysis of the sensorgrams in Fig. S1. [b]The values for all kinetic parameters are expressed as the mean ± 1 SD (n=2).

Table III. Affinity constants for fusion toxins interacting with human and mouse serum albumin.[a]

	Human serum albumin			Mouse serum albumin		
Fusion toxin	$k_a/10^5$ (1/Ms)[b]	$k_d/10^{-4}$ (1/s)[b]	$K_D/10^{-9}$ (M)[b]	$k_a/10^5$ (1/Ms)[b]	$k_d/10^{-3}$ (1/s)[b]	$K_D/10^{-9v}$ (M)[b]
$ADAPT_6$-ABD-PE25	1.86±0.01	2.01±0.01	1.08±0.01	2.91±0.06	1.90±0.01	6.53±0.08
$ADAPT_6$-ABD-PE38X8	1.72±0.05	3.69±0.23	2.15±0.20	3.95±0.20	2.23±0.15	5.63±0.09
Z_{Taq}-ABD-PE25	1.82±0.03	3.2±0.17	1.76±0.07	4.21±0.35	1.49±0.01	3.55±0.33

[a]The values for the kinetic parameters are derived from analysis of the sensorgrams in Fig. S2. [b]The values for all kinetic parameters are expressed as mean ± 1 SD (n=2).

3 orders of magnitude for the 3 cell lines with a high HER2 expression.

All fusion toxins demonstrated substantially weaker cytotoxic potential for A549 cells with a moderate HER2 expression (Fig. 2A). The IC_{50} values were 15,000 pM with a 95% confidence interval between 13,000 and 19,000 pM ($ADAPT_6$-ABD-PE25) and 5,600 pM with a 95% confidence interval between 4,500 and 7,300 pM ($ADAPT_6$-ABD-PE38X8). The relative viability of A549 cells at the concentrations used was not affected to such an extent by Z_{Taq}-ABD-PE25 that the IC_{50} values could be measured.

Rescue of SKOV3 viability. One of the $ADAPT_6$-containing variants, $ADAPT_6$-ABD-PE25, was investigated further. Its dependence on HER2 availability for activity was determined by treating SKOV3 cells with a constant concentration of $ADAPT_6$-ABD-PE25 in the presence of increasing concentrations of free $ADAPT_6$ to potentially block receptor binding sites on HER2, preventing interaction with the fusion toxin. As shown in Fig. 2B, SKOV3 cell viability was gradually increased by an increase in the concentration of free $ADAPT_6$ and full viability was found at 1,000-fold excess, strongly indicating that $ADAPT_6$-ABD-PE25 is dependent on specific interaction with HER2 for intoxication. Transferrin, which does not interact with HER2, was used as a control. It was added in the same molar excess (1,000-fold) as free $ADAPT_6$ and was found to not affect the efficiency of $ADAPT_6$-ABD-PE25 (Fig. 2C). Free $ADAPT_6$ and transferrin did not affect cell viability when used alone.

Influence of contact time. The capability of fusion toxins to deliver their cytotoxic effect is dependent on their ability to be internalized by the target cell, which in turn is dependent on the contact time. To examine the relationship between fusion toxin contact time and cell viability, SKOV3 cells were incubated with a constant concentration of $ADAPT_6$-ABD-PE25 for different times after which the toxin was removed. The viability decreased with increasing contact time (Fig. 2D) for the duration of the experiment (24 h). The half-maximum effect was reached after approximately 30 min.

Biodistribution in mice. To investigate biodistribution, the fusion toxins were radiolabeled with ^{111}In, resulting in conjugates with high radiochemical purity (>95%) and high stability during EDTA challenge (Table SI). The conjugates were subsequently injected into NMRI mice followed by measurement of radioactive uptake in different organs (Table IV). As a positive control, the HER2-specific fusion toxin $Z_{HER2:2891}$-ABD-PE38X8 was included. This fusion toxin has previously been thoroughly characterized (11,12), where the targeting domain $Z_{HER2:2891}$ is a size-matched control with a fold similar to $ADAPT_6$. The comparison of the values at 4 and 24 h revealed that the uptake in the different organs of all conjugates followed a similar pattern, but with lower values at 24 h. The comparison of $ADAPT_6$-ABD-PE25 and ADAPT6-ABD-PE38X8 at 24 h post-injection (p.i.) revealed a 5-fold higher uptake in liver (32.0±5.0 vs. 6.0±1.0 %ID/g) and a 4-fold lower in kidney (11.0±1.0 vs. 46.0±2.0 %ID/g) for the toxin containing PE25. $ADAPT_6$-ABD-PE25 also had a significantly lower uptake in blood at both time points compared to $ADAPT_6$-ABD-PE38X8. By comparing $ADAPT_6$-ABD-PE25 with $ADAPT_6$-PE25, a profound impact of the addition of ABD on half-life in circulation was observed. At 4 h, the uptake in blood was significantly higher (3.2±0.1 %ID/g) for the compound with an ABD compared to 0.2±0.1 %ID/g for the variant lacking ABD. The uptake in

Table IV. Comparative biodistribution of the ^{111}In-labeled fusion toxins in mice 4 and 24 h following intravenous injection.[a]

	$Z_{HER2:2891}$-ABD-PE38X8	$ADAPT_6$-ABD-PE38X8	$ADAPT_6$-ABD-PE25	$ADAPT_6$-PE25
At 4 h post-injection				
Blood	6.0±0.7[c,d,e]	9.0±0.7[d,e]	3.2±0.1[e]	0.2±0.1
Heart	2.8±0.3[d,e]	3.0±0.8	1.1±0.2	0.7±0.1
Lung	2.4±1.3	3.3±0.4[d]	1.3±0.1[e]	3.1±0.4
Sal. gland	1.0±0.2[e]	1.5±0.2[d,e]	0.7±0.2	0.2±0.1
Liver	23.0±2.0[c]	9.0±0.4[d,e]	43.0±7.0	33.0±6.0
Spleen	9.0±1.0[c]	3.3±0.3[d]	19.0±4.0	7.0±3.0
Pancreas	0.6±0.1	0.9±0.2	0.4±0.1	0.3±0.2
Stomach	1.1±0.4	1.0±0.1[e]	0.5±0.2	0.2±0.1
Kidney	8.0±4.0[c]	58.0±3.0[d,e]	13.0±1.0[e]	28.0±4.0
Colon	0.9±0.1[c,e]	1.1±0.1[e]	0.6±0.3	0.3±0.1
Skin	1.0±0.1[d,e]	1.8±0.3[d,e]	0.6±0.1[e]	0.2±0.1
Muscle	0.6±0.1[d]	0.7±0.1[d,e]	0.3±0.1	0.3±0.1
Bone	1.9±0.2	1.3±0.1	1.1±0.3	1.6±0.4
GI tract[b]	4.2±0.5	5.2±0.3	6.9±4.4[e]	2.6±0.5
Carcass[b]	16.0±1.0[d,e]	22.0±1.8[b,c]	4.0±3.0	7.0±1.0
At 24 h post-injection				
Blood	2.0±0.1e	1.8±0.1[d,e]	1.3±0.2[e]	0.1±0.1
Heart	1.8±0.2[c,d,e]	1.0±0.1[e]	0.7±0.2	0.5±0.1
Lung	1.7±0.2[c]	1.0±0.2	0.8±0.1	2.6±0.8
Sal. gland	1.2±0.1[c,d,e]	0.7±0.1[e]	0.6±0.1[e]	0.2±0.1
Liver	22.0±2.0[c]	6.0±1.0[d,e]	32.0±5.0	27.0±3.0
Spleen	9.0±2.0[c,e]	2.2±0.4[d]	11.4±1.3[e]	4.0 ±1.0
Pancreas	0.6±0.1e	0.4±0.1[e]	0.4±0.2	0.1±0.1
Stomach	0.7±0.1[d,e]	0.5±0.1[e]	0.4±0.2	0.2±0.1
Kidney	9.0±1.0[c,e]	46.0±2.0[d,e]	11.0±1.0[e]	19.0±1.0
Colon	0.9±0.1[c,d]	0.3±0.1	0.3±0.1	0.3±0.2
Skin	1.2±0.1[e]	1.3±0.3[e]	0.7±0.2[e]	0.1±0.1
Muscle	0.5±0.1[d,e]	0.4±0.1	0.3±0.1	0.2±0.1
Bone	1.8±0.3[c]	0.7±0.2[e]	0.8±0.2	1.6±0.2
GI tract[a]	2.7±0.7	1.1±0.2	1.0±0.3	0.6±0.2
Carcass[b]	13.3±1.4[d,e]	11.5±1.6[d,e]	7.0±1.0	5.4±0.5

[a]The measured radioactivity of different organs is expressed as %ID/g, and presented as an average value from 4 animals ± 1 SD. [b]Data for GI tract with content and carcass are presented as %ID per whole sample. Data were assessed by one-way ANOVA with Bonferroni's post hoc multiple comparisons test in order to determine significant differences between groups ($P<0.05$) at the same time point. No statistical analysis of values obtained for the same construct in the same organ at the two time-points was performed. [c]$P<0.05$ vs. $ADAPT_6$-ABD-PE38X8. [d]$P<0.05$ vs. $ADAPT_6$-ABD-PE25. [e]$P<0.05$ vs. $ADAPT_6$-PE25.

kidney of $ADAPT_6$-ABD-PE25 was also decreased compared to $ADAPT_6$-PE25 (11.0±1.0 vs. 19.0±1.0 %ID/g at 24 h p.i.). However, the uptake in liver remained similar for both constructs (27.0±3.0 vs. 32.0±5.0 %ID/g at 24 h p.i).

Discussion

In this study, we demonstrated that an ADAPT, specifically interacting with HER2, can be expressed as a fusion to different truncated variants of ETA, leading to potent fusion toxins with high specificity for HER2 expressing cells. The fusion toxins could be expressed in a soluble form in *E. coli* and easily purified to homogeneity. By contrast, PE38-derived immunotoxins, where immunoglobulin-based targeting domains are utilized, may require more advanced host cells or a refolding step during purification (37). Soluble expression in a simple prokaryotic host cell for ADAPT-based fusion toxins may be an important cost-of-goods advantage in a potential future commercial manufacturing process, when large amounts of GMP-grade (good manufacturing practice-grade) material is needed.

ADAPTs comprise a class of novel engineered affinity proteins and they are some of the smallest folded affinity proteins (Mw of 5 kDa). The size is one important parameter to consider during development of protein therapeutics for intended cancer therapy, and it has previously been shown that a smaller size leads to more efficient accumulation in solid tumors (38). This

is a consequence of the typically inefficient lymphatic drainage and an increased interstitial pressure in solid tumors, leading to that the rate of penetration is mostly dependent on diffusivity, and hence the size, of the protein therapeutic (39,40). Inefficient penetration and distribution in the tumor may lead to untargeted portions of the tumor and portions where the concentration of the therapeutic molecule is low. This may in turn lead to selection for resistant clones. One of the fusion toxins investigated in this study, $ADAPT_6$-PE25 (Mw of 33 kDa), is one of the smallest fusion toxins or immunotoxins created.

However, since $ADAPT_6$-PE25 is also considerably smaller than the cut-off of the glomerular filter in the kidneys (ca 60 kDa), its blood retention was low, likely a consequence of quick excretion to urine. A slightly larger version, $ADAPT_6$-ABD-PE25, including an ABD for *in vivo* half-life extension was therefore also evaluated (Mw of 41 kDa). This version was found to interact strongly with MSA and HSA, and should thus form a 108 kDa complex with serum albumin *in vivo*, well above the cut-off of the glomerular filtration. Indeed, the blood retention at both 4 and 24 h p.i. was significantly higher for the fusion toxin including the ABD. In addition to an increase in size, the interaction with albumin extends serum half-life by 'piggybacking' on the FcRn-dependent intracellular rescue system for serum albumin (41).

The internalization of free $ADAPT_6$ has previously been investigated in SKOV3 cells, and it was found that it is indeed internalized (36). In this study, the cells were efficiently killed by the fusion toxins including $ADAPT_6$, which act on cytosolic elongation factor 2, suggesting that also the fusion toxins are efficiently internalized.

Previously, fusion toxins utilizing an affibody molecule ($Z_{HER2:2891}$) with specific affinity for HER2 have been evaluated (11,12). This targeting domain is slightly larger than $ADAPT_6$ (58 compared to 46 amino acids), but with a similar, anti-parallel 3-helix fold. $Z_{HER2:2891}$ has a higher affinity for HER2, which was reflected in the affinities of the fusion toxins for HER2, $Z_{HER2:2891}$-ABD-PE38X8 had an equilibrium dissociation constant of 5 nM (11) compared to $ADAPT_6$-ABD-PE38X8 which had an equilibrium dissociation constant of 26 nM. *In vitro*, $ADAPT_6$-ABD-PE38X8 was 6- to 7-fold less potent compared to $Z_{HER2:2891}$-ABD-PE38X8. The contact time needed to reach 50% viability (Fig. 2D) was also longer for $ADAPT_6$-ABD-PE38X8 (30 min) compared to $Z_{HER2:2891}$-ABD-PE38X8 (15 min). Both of the above could be a consequence of the weaker affinity of $ADAPT_6$-ABD-PE38X8 for HER2. Compared to the non-targeting control, Z_{Taq}-ABD-PE25, the cytotoxic potential of the 3 $ADAPT_6$ containing fusion toxins had 2 to 3 orders of magnitude lower IC_{50} values on the cell lines with a high HER2 expression, which translates into a large therapeutic window. A strong affinity is desired for efficient receptor binding, but too strong affinity may hamper tumor penetration (42). The balance between binding-strength and tumor accumulation is more important for constructs smaller than the pores of the glomerular filter in the kidneys and is thus more important for $ADAPT_6$-PE25 than for the constructs including the ABD.

Two different truncated versions of ETA were investigated in this study, PE38X8 and PE25, which have both been found to retain a similar cytotoxic potential as the parental PE38 toxin (10,14). In the context of a C-terminal fusion to $ADAPT_6$-ABD, the cytotoxicity was found to be slightly weaker for the PE25 version on the cell lines with a high HER2 expression: SKBR3, AU565 and SKOV3 cells. For the moderate-expressing cell line, A549, the PE38X8-containing fusion toxin was 4-fold more potent than the PE25-containing fusion toxin (IC_{50} 3.4 nM versus 15 nM). However, the slight loss of cytotoxic potential of $ADAPT_6$-ABD-PE25 on A549 cells may be compensated by other favorable properties; its smaller size may lead to increased tumor accumulation and its deimmunizing mutations should decrease formation of neutralizing antibodies *in vivo* (14).

The biodistribution of the ABD-containing fusion toxins revealed a significantly higher accumulation in blood at both 4 h and 24 h post injection compared to $ADAPT_6$-PE25, clearly demonstrating the circulation half-life extension effect of the ABD. Surprisingly, $ADAPT_6$-ABD-PE25 was found to have a lower blood retention than $ADAPT_6$-ABD-PE38X8, indicating a possible hampering of the serum albumin interaction, even though the affinity for mouse serum albumin was similar in the biosensor experiment (Table III). It has to be noted that the biosensor is an artificial system, and interaction conditions with immobilized albumin may not exactly mimic the *in vivo* conditions. This indicates that animal studies are required for a proper evaluation. Another factor leading to the reduced blood retention of $ADAPT_6$-ABD-PE25 may be an elevated sequestering by the liver. The hepatic uptake of both $ADAPT_6$-ABD-PE25 and $ADAPT_6$-PE25 was several-fold higher than the uptake of $ADAPT_6$-ABD-PE38X8. A lower liver uptake of $ADAPT_6$-ABD-PE38X8 may also be associated with a lower hepatic toxicity, although animal studies have demonstrated that an uptake of ETA-derivatives in liver was well tolerated (17). All 4 constructs accumulated in the kidneys, although to varying extents. Since a radionuclide with residualizing properties is used, the accumulation measured in the kidneys is proportional to the sum of the uptake and lysosomal degradation during the course of the whole experiment. Generally, the uptake of proteins from primary urine in the kidneys is mainly carried out by the megalin/cubulin complex of receptors (43). This complex recognizes a variety of different ligands, including vitamins and proteins. The accumulation of radioactivity in the kidneys of the 4 constructs is dependent on several parameters, including the affinity between the construct and the megalin/cubulin complex outside of the cells, the potential triggering of endocytosis and the release inside the endosomes of the kidney cells. In addition, the rate at which the peptide linker between $ADAPT_6$ and the toxin is cleaved may also influence transport to the lysosomes for degradation. The comparison of $ADAPT_6$ and $Z_{HER2:2891}$ as targeting domains in the context of an N-terminal fusion to ABD-PE38X8 (Table IV), revealed that blood retention was increased, accumulation in liver and spleen was decreased, and accumulation in kidney was increased when employing $ADAPT_6$. Apparently, the targeting part of a fusion toxin may have a substantial influence on biodistribution.

In conclusion, it was found that fusion toxins consisting of a HER2-targeting ADAPT coupled to ETA-derived cytotoxic domains, are highly potent agents for specific killing of HER2-expressing cells. Inclusion of an ABD was found to prolong the residence time in blood, which increases the

bioavailability. On the whole, the findings motivate further pre-clinical and clinical evaluations.

Acknowledgements

The authors are grateful to Mr. Andreas Hober (Department of protein science, KTH Royal institute of technology, Stockholm, Sweden) for providing expert technical assistance.

Funding

This study was financially supported by a grant from the Swedish cancer foundation (Cancerfonden; CAN 2015/746) and Vinnova (grant no. 2016-04060). The funding bodies did not participate in the design of the study, collection, analysis or interpretation of data or writing of the manuscript.

Availability of data and materials

All data and materials included in this article are available from the corresponding author upon reasonable request.

Authors' contributions

HL, SL, MA, AO, VT, SH and TG designed the study and experiments. HL, HD, MA, JG, AO and VT performed the experiments. HL, HD, MA, JG, AO, VT, SH and TG analyzed and interpreted the data. SL, MA, AO, VT, SH and TG wrote the manuscript. All authors have read and approved the final version of the manuscript.

Ethics approval and consent to participate

The animal experiments were planned and performed in accordance with Sweden's national legislation on laboratory animals' protection. The animal studies were approved by the local ethics committee for animal research in Uppsala, Sweden.

Patient consent for publication

Not applicable.

Competing interests

The authors declare that they have no competing interests.

References

1. Alewine C, Hassan R and Pastan I: Advances in anticancer immunotoxin therapy. Oncologist 20: 176-185, 2015.
2. Akbari B, Farajnia S, Ahdi Khosroshahi S, Safari F, Yousefi M, Dariushnejad H and Rahbarnia L: Immunotoxins in cancer therapy: Review and update. Int Rev Immunol 36: 207-219, 2017.
3. Kreitman RJ, Dearden C, Zinzani PL, Delgado J, Karlin L, Robak T, Gladstone DE, le Coutre P, Dietrich S, Gotic M, *et al*: Moxetumomab pasudotox in relapsed/refractory hairy cell leukemia. Leukemia 32: 1768-1777, 2018.
4. Martin-Killias P, Stefan N, Rothschild S, Plückthun A and Zangemeister-Wittke U: A novel fusion toxin derived from an EpCAM-specific designed ankyrin repeat protein has potent antitumor activity. Clin Cancer Res 17: 100-110, 2011.
5. Prince HM, Duvic M, Martin A, Sterry W, Assaf C, Sun Y, Straus D, Acosta M and Negro-Vilar A: Phase III placebo-controlled trial of denileukin diftitox for patients with cutaneous T-cell lymphoma. J Clin Oncol 28: 1870-1877, 2010.
6. Onda M, Nagata S, FitzGerald DJ, Beers R, Fisher RJ, Vincent JJ, Lee B, Nakamura M, Hwang J, Kreitman RJ, *et al*: Characterization of the B cell epitopes associated with a truncated form of *Pseudomonas* exotoxin (PE38) used to make immunotoxins for the treatment of cancer patients. J Immunol 177: 8822-8834, 2006.
7. Liu W, Onda M, Lee B, Kreitman RJ, Hassan R, Xiang L and Pastan I: Recombinant immunotoxin engineered for low immunogenicity and antigenicity by identifying and silencing human B-cell epitopes. Proc Natl Acad Sci USA 109: 11782-11787, 2012.
8. Onda M, Beers R, Xiang L, Lee B, Weldon JE, Kreitman RJ and Pastan I: Recombinant immunotoxin against B-cell malignancies with no immunogenicity in mice by removal of B-cell epitopes. Proc Natl Acad Sci USA 108: 5742-5747, 2011.
9. Mazor R, Vassall AN, Eberle JA, Beers R, Weldon JE, Venzon DJ, Tsang KY, Benhar I and Pastan I: Identification and elimination of an immunodominant T-cell epitope in recombinant immunotoxins based on *Pseudomonas* exotoxin A. Proc Natl Acad Sci USA 109: E3597-E3603, 2012.
10. Onda M, Beers R, Xiang L, Nagata S, Wang Q-C and Pastan I: An immunotoxin with greatly reduced immunogenicity by identification and removal of B cell epitopes. Proc Natl Acad Sci USA 105: 11311-11316, 2008.
11. Liu H, Seijsing J, Frejd FY, Tolmachev V and Gräslund T: Target-specific cytotoxic effects on HER2-expressing cells by the tripartite fusion toxin $Z_{HER2:2891}$-ABD-PE38X8, including a targeting affibody molecule and a half-life extension domain. Int J Oncol 47: 601-609, 2015.
12. Altai M, Liu H, Orlova A, Tolmachev V and Gräslund T: Influence of molecular design on biodistribution and targeting properties of an Affibody-fused HER2-recognising anticancer toxin. Int J Oncol 49: 1185-1194, 2016.
13. Weldon JE, Skarzynski M, Therres JA, Ostovitz JR, Zhou H, Kreitman RJ and Pastan I: Designing the furin-cleavable linker in recombinant immunotoxins based on *Pseudomonas* exotoxin A. Bioconjug Chem 26: 1120-1128, 2015.
14. Mazor R, Onda M, Park D, Addissie S, Xiang L, Zhang J, Hassan R and Pastan I: Dual B- and T-cell de-immunization of recombinant immunotoxin targeting mesothelin with high cytotoxic activity. Oncotarget 7: 29916-29926, 2016.
15. Wurch T, Pierré A and Depil S: Novel protein scaffolds as emerging therapeutic proteins: From discovery to clinical proof-of-concept. Trends Biotechnol 30: 575-582, 2012.
16. Zielinski R, Lyakhov I, Jacobs A, Chertov O, Kramer-Marek G, Francella N, Stephen A, Fisher R, Blumenthal R and Capala J: Affitoxin - a novel recombinant, HER2-specific, anticancer agent for targeted therapy of HER2-positive tumors. J Immunother 32: 817-825, 2009.
17. Zielinski R, Lyakhov I, Hassan M, Kuban M, Shafer-Weaver K, Gandjbakhche A and Capala J: HER2-affitoxin: A potent therapeutic agent for the treatment of HER2-overexpressing tumors. Clin Cancer Res 17: 5071-5081, 2011.
18. Simon M, Stefan N, Borsig L, Plückthun A and Zangemeister-Wittke U: Increasing the antitumor effect of an EpCAM-targeting fusion toxin by facile click PEGylation. Mol Cancer Ther 13: 375-385, 2014.
19. Ham S, Min KA, Yang JW and Shin MC: Fusion of gelonin and anti-insulin-like growth factor-1 receptor (IGF-1R) affibody for enhanced brain cancer therapy. Arch Pharm Res 40: 1094-1104, 2017.
20. Nilvebrant J and Hober S: The albumin-binding domain as a scaffold for protein engineering. Comput Struct Biotechnol J 6: e201303009, 2013.
21. Alm T, Yderland L, Nilvebrant J, Halldin A and Hober S: A small bispecific protein selected for orthogonal affinity purification. Biotechnol J 5: 605-617, 2010.
22. Nilvebrant J, Åstrand M, Löfblom J and Hober S: Development and characterization of small bispecific albumin-binding domains with high affinity for ErbB3. Cell Mol Life Sci 70: 3973-3985, 2013.
23. Nilvebrant J, Åstrand M, Georgieva-Kotseva M, Björnmalm M, Löfblom J and Hober S: Engineering of bispecific affinity proteins with high affinity for ERBB2 and adaptable binding to albumin. PLoS One 9: e103094, 2014.
24. Hynes NE and MacDonald G: ErbB receptors and signaling pathways in cancer. Curr Opin Cell Biol 21: 177-184, 2009.

25. Tai W, Mahato R and Cheng K: The role of HER2 in cancer therapy and targeted drug delivery. J Control Release 146: 264-275, 2010.
26. Slamon DJ, Leyland-Jones B, Shak S, Fuchs H, Paton V, Bajamonde A, Fleming T, Eiermann W, Wolter J, Pegram M, *et al*: Use of chemotherapy plus a monoclonal antibody against HER2 for metastatic breast cancer that overexpresses HER2. N Engl J Med 344: 783-792, 2001.
27. von Minckwitz G, Procter M, de Azambuja E, Zardavas D, Benyunes M, Viale G, Suter T, Arahmani A, Rouchet N, Clark E, *et al*; APHINITY Steering Committee and Investigators: Adjuvant pertuzumab and trastuzumab in early HER2-positive breast cancer. N Engl J Med 377: 122-131, 2017.
28. Verma S, Miles D, Gianni L, Krop IE, Welslau M, Baselga J, Pegram M, Oh DY, Diéras V, Guardino E, *et al*; EMILIA Study Group: Trastuzumab emtansine for HER2-positive advanced breast cancer. N Engl J Med 367: 1783-1791, 2012.
29. Lindbo S, Garousi J, Åstrand M, Honarvar H, Orlova A, Hober S and Tolmachev V: Influence of histidine-containing tags on the biodistribution of ADAPT scaffold proteins. Bioconjug Chem 27: 716-726, 2016.
30. Garousi J, Lindbo S, Nilvebrant J, Åstrand M, Buijs J, Sandström M, Honarvar H, Orlova A, Tolmachev V and Hober S: ADAPT, a novel scaffold protein-based probe for radionuclide imaging of molecular targets that are expressed in disseminated cancers. Cancer Res 75: 4364-4371, 2015.
31. Hopp J, Hornig N, Zettlitz KA, Schwarz A, Fuss N, Müller D and Kontermann RE: The effects of affinity and valency of an albumin-binding domain (ABD) on the half-life of a single-chain diabody-ABD fusion protein. Protein Eng Des Sel 23: 827-834, 2010.
32. Makrides SC, Nygren PÅ, Andrews B, Ford PJ, Evans KS, Hayman EG, Adari H, Uhlén M and Toth CA: Extended in vivo half-life of human soluble complement receptor type 1 fused to a serum albumin-binding receptor. J Pharmacol Exp Ther 277: 534-542, 1996.
33. Orlova A, Jonsson A, Rosik D, Lundqvist H, Lindborg M, Abrahmsen L, Ekblad C, Frejd FY and Tolmachev V: Site-specific radiometal labeling and improved biodistribution using ABY-027, a novel HER2-targeting affibody molecule-albumin-binding domain fusion protein. J Nucl Med 54: 961-968, 2013.
34. Jonsson A, Dogan J, Herne N, Abrahmsén L and Nygren PÅ: Engineering of a femtomolar affinity binding protein to human serum albumin. Protein Eng Des Sel 21: 515-527, 2008.
35. Gunneriusson E, Nord K, Uhlén M and Nygren P: Affinity maturation of a Taq DNA polymerase specific affibody by helix shuffling. Protein Eng 12: 873-878, 1999.
36. Garousi J, Lindbo S, Honarvar H, Velletta J, Mitran B, Altai M, Orlova A, Tolmachev V and Hober S: Influence of the N-terminal composition on targeting properties of radiometal-labeled anti-HER2 scaffold protein $ADAPT_6$. Bioconjug Chem 27: 2678-2688, 2016.
37. Pastan I, Beers R and Bera TK: Recombinant immunotoxins in the treatment of cancer. Methods Mol Biol 248: 503-518, 2004.
38. Zahnd C, Kawe M, Stumpp MT, de Pasquale C, Tamaskovic R, Nagy-Davidescu G, Dreier B, Schibli R, Binz HK, Waibel R, *et al*: Efficient tumor targeting with high-affinity designed ankyrin repeat proteins: Effects of affinity and molecular size. Cancer Res 70: 1595-1605, 2010.
39. Thurber GM, Schmidt MM and Wittrup KD: Antibody tumor penetration: Transport opposed by systemic and antigen-mediated clearance. Adv Drug Deliv Rev 60: 1421-1434, 2008.
40. Heldin CH, Rubin K, Pietras K and Östman A: High interstitial fluid pressure - an obstacle in cancer therapy. Nat Rev Cancer 4: 806-813, 2004.
41. Roopenian DC and Akilesh S: FcRn: The neonatal Fc receptor comes of age. Nat Rev Immunol 7: 715-725, 2007.
42. Schmidt MM and Wittrup KD: A modeling analysis of the effects of molecular size and binding affinity on tumor targeting. Mol Cancer Ther 8: 2861-2871, 2009.
43. Nielsen R, Christensen EI and Birn H: Megalin and cubilin in proximal tubule protein reabsorption: From experimental models to human disease. Kidney Int 89: 58-67, 2016.